

Inclusive electron scattering from nuclei at $x \approx 1$

J. Arrington,¹ P. Anthony,² R. G. Arnold,³ E. J. Beise,^{1,a} J. E. Belz,^{1,b} P. E. Bosted,³ H.-J. Bulten,⁴ M. S. Chapman,⁵ K. P. Coulter,^{6,c} F. Dietrich,² R. Ent,^{5,d} M. Epstein,⁷ B. W. Filippone,¹ H. Gao,^{1,e} R. A. Gearhart,⁸ D. F. Geesaman,⁶ J.-O. Hansen,⁵ R. J. Holt,⁶ H. E. Jackson,⁶ C. E. Jones,^{4,f} C. E. Keppel,^{3,g} E. R. Kinney,⁹ S. Kuhn,^{10,h} K. Lee,⁵ W. Lorenzon,^{1,i} A. Lung,^{3,j} N. C. R. Makins,⁵ D. J. Margaziotis,⁷ R. D. McKeown,¹ R. G. Milner,⁵ B. Mueller,¹ J. Napolitano,¹¹ J. Nelson,^{5,k} T. G. O'Neill,^{1,f} V. Papavassiliou,^{6,l} G. G. Petratos,^{8,m} D. H. Potterveld,⁶ S. E. Rock,³ M. Spengos,³ Z. M. Szalata,³ L. H. Tao,³ K. van Bibber,² J. F. J. van den Brand,⁴ J. L. White,³ D. Winter,^{5,n} and B. Zeidman⁶

¹California Institute of Technology, Pasadena, California 91125

²Lawrence Livermore National Laboratory, Livermore, California 94550

³American University, Washington, D.C. 20016

⁴University of Wisconsin, Madison, Wisconsin 53706

⁵Massachusetts Institute of Technology, Cambridge, Massachusetts 02139

⁶Argonne National Laboratory, Argonne, Illinois 60439

⁷California State University, Los Angeles, California 90032

⁸Stanford Linear Accelerator Center, Stanford, California 94309

⁹University of Colorado, Boulder, Colorado 80309

¹⁰Stanford University, Stanford, California 94305

¹¹Rensselaer Polytechnic Institute, Troy, New York 12180

(Received 6 March 1995)

The inclusive $A(e, e')$ cross section for $x \approx 1$ was measured on ²H, C, Fe, and Au for momentum transfers Q^2 from 1 to 6.8 (GeV/c)². The scaling behavior of the data was examined in the region of transition from y scaling to x scaling. Throughout this transitional region, the data exhibit ξ scaling, reminiscent of the Bloom-Gilman duality seen in free nucleon scattering. [S0556-2813(96)01705-0]

PACS number(s): 25.30.Fj, 13.60.Hb

In inclusive electron scattering, scaling functions are important in the study of constituent substructure and interactions. Scaling is typically a sign that a simple reaction mechanism dominates the process, allowing one to extract

information on structure in a model independent way. The most familiar scaling occurs in the limit of large ν and Q^2 , where ν is the energy transfer and $-Q^2 = q_\mu^2$ is the square of the four-momentum transfer. In this limit the nucleon deep inelastic structure functions $MW_1(\nu, Q^2)$ and $\nu W_2(\nu, Q^2)$ become functions only of the Bjorken $x = Q^2/2M\nu$, where M is the nucleon mass. In this limit, x can be interpreted as the fraction of the nucleon's longitudinal momentum carried by the struck quark, and MW_1 and νW_2 are related to the quark longitudinal momentum distribution. Violations of Bjorken scaling in the free nucleon exist at low Q^2 due to target mass and higher-twist effects. To correct for the effects of target mass at finite Q^2 , the Nachtmann variable $\xi = 2x/[1 + (1 + 4M^2x^2/Q^2)^{1/2}]$ has been used in place of x . This has been shown to be the correct variable in which to study the logarithmic QCD scaling violations in the nucleon [1]. A more recent work by Gurvitz proposes a new scaling variable that includes parton confinement effects [2].

A similar case exists for quasielastic scattering from a nucleon in a nucleus. At high momentum transfer, the "reduced" cross section was predicted [3], and later observed [4] to exhibit scaling in the variable $y(q, \nu)$ [in a simple relativistic approximation $y = (2M\nu + \nu^2 - q^2)/2q$, where q is the momentum transfer]. In the simplest picture of y scaling, the electron-nucleus cross section is divided by the elastic nucleon cross section, leaving a universal function $F(y)$ which is independent of Q^2 in the plane wave impulse approximation. In the scaling limit, y can be interpreted as the nucleon's initial momentum along the momentum transfer direction, and $F(y)$ is related to the nucleon's momentum

^aPresent address: University of Maryland, College Park, Maryland 20742.

^bPresent address: University of Colorado, Boulder, Colorado 80309.

^cPresent address: University of Michigan, Ann Arbor, Michigan 48109.

^dPresent address: CEBAF, Newport News, Virginia 23606.

^ePresent address: University of Illinois at Urbana-Champaign, Urbana, Illinois 61801.

^fPresent address: Argonne National Laboratory, Argonne, Illinois 60439.

^gPresent address: Virginia Union University, Richmond, Virginia 23220.

^hPresent address: Old Dominion University, Norfolk, Virginia 23529.

ⁱPresent address: University of Pennsylvania, Philadelphia, Pennsylvania 19104.

^jPresent address: California Institute of Technology, Pasadena, California 91125.

^kPresent address: SLAC, Stanford, California 94309.

^lPresent address: Illinois Institute of Technology, Chicago, Illinois 60616.

^mPresent address: Kent State University, Kent, Ohio 44242.

ⁿPresent address: Columbia University, New York, New York 10027.

distribution in the nucleus. Thus, y plays a similar role for nucleons in a nucleus as x does for quarks in a nucleon.

In the limit of high Q^2 , the scaling variables x , y , and ξ are related. In the parton model, ξ replaces x as the scaling variable when the target mass is not neglected. At large Q^2 , ξ can also be expressed as a function only of y (with the leading scale-breaking term M^2/Q^2) [5]. There may also be a relationship between quasielastic and inelastic scattering at more modest momentum transfers. In the case of the free nucleon, Bloom and Gilman [6] discovered that the resonance peaks in the structure function have the same Q^2 behavior as the deep inelastic contribution when viewed as a function of ω' , a modified version of the Bjorken scaling variable. It was later shown [7] that this connection between the high Q^2 structure function and the resonance form factors, called local duality, was expected from perturbative QCD and should be valid for the nucleon elastic peak as well as the resonance peaks if the structure function is analyzed in terms of ξ . When the structure function is viewed as a function of ξ , the elastic and resonance peaks have the same Q^2 behavior as the deep inelastic structure function. The magnitude of the elastic and resonance peaks decrease rapidly with Q^2 , but move to higher ξ , keeping a nearly constant strength with respect to the deep inelastic structure function, which falls with ξ . Thus the strong Q^2 dependence of the higher twist effects (the elastic and resonance peaks) is removed when the structure function is averaged over a range in ξ . In the case of electron scattering from a nucleus, the Fermi motion can perform this ‘‘averaging’’ of the structure function. Thus, when examining νW_2^A as a function of ξ , scaling may be observed at lower momentum transfers where x scaling is not yet valid due to the quasielastic contribution.

Scaling in inclusive scattering from nuclei (He, C, Fe, and Au) was examined in a previous measurement [8, 5] for Q^2 values of 0.3–3.1 (GeV/c)². For these values of momentum transfer, where the quasielastic contribution dominates the cross section, the data exhibit y scaling for $y < 0$ ($x > 1$). The positive y values represent the high energy-transfer side of the quasielastic peak where the y scaling breaks down due to the increasing inelastic contribution at higher Q^2 . This same experiment examined x and ξ scaling in the nucleus [5]. For low values of x , the structure function νW_2 is a function only of x , as predicted. For values of x near or above 1, scaling was not observed due to the contribution of quasielastic scattering. If one examines the structure function vs the Nachtmann variable ξ , a scaling behavior is suggested; at lower ξ , the data are nearly independent of Q^2 , while at higher ξ , the data approach a universal curve. More recent data at higher Q^2 show the same approach to scaling for inclusive scattering from aluminum [9]. The beginning of scaling in this region suggests that ξ scaling is not only applicable to deep inelastic scattering, but is also connected to quasielastic scattering and y scaling. Here we examine scaling in the transition region from quasielastic to deep inelastic scattering, to further study the connection between ξ scaling and y scaling.

The data presented here are from the NE18 experiment [10, 11], a coincidence $A(e, e'p)$ measurement performed in End Station A at the SLAC Nuclear Physics Facility

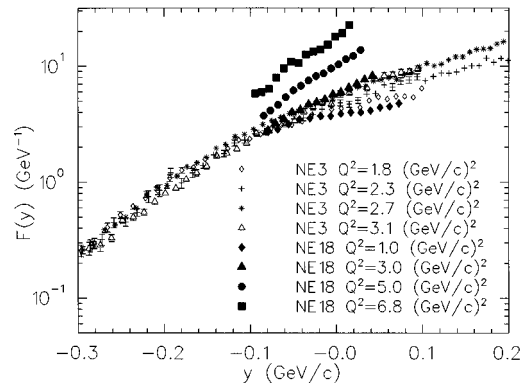


FIG. 1. $F(y)$ vs y for iron for the present experiment and the previous NE3 measurement. Errors in the new data (solid points) are dominated by a 4% systematic error, but are smaller than the points shown.

(NPAS). Electron singles were recorded as well as the electron-proton coincidences and this data was analyzed to extract the inclusive cross section. Scattering was measured from cryogenic liquid ¹H and ²H targets and solid C, Fe, and Au targets with beam energies of 2.02, 3.19, 4.21, and 5.12 GeV, at angles of 35.5°, 47.4°, 53.4°, and 56.6°, respectively [$Q^2=1, 3, 5, \text{ and } 6.8 \text{ (GeV/c)}^2$]. The scattered electrons were detected in the SLAC 1.6 GeV/c spectrometer. The pion rate in the spectrometer was up to 500 times the electron rate for runs on Au at the highest Q^2 . A CO₂ gas Čerenkov counter and lead glass shower counter were used to eliminate the pions. Tight cuts were used in the final analysis, resulting in a pion rejection of 15 000 to 1, while maintaining an electron efficiency of 90%.

In order to extract the cross section, corrections for spectrometer acceptance, detector efficiencies, data acquisition deadtimes, and radiative corrections were applied to the data. The acceptance was determined using a Monte Carlo model of the spectrometer, and deadtime corrections were measured on a run-by-run basis. Radiative corrections were applied using an iterative procedure following the formulas of Stein *et al.* [12], which are based on the work of Mo and Tsai [13] and Tsai [14]. Radiative effects were calculated for a model cross section and the result was compared to the data to determine a smooth correction to the model. The ‘‘corrected’’ model was then used in place of the original model cross section, and the procedure repeated until the radiated model was consistent with the data. The model dependence of the radiative correction procedure was tested by varying the initial model cross section. We also compared the radiatively corrected cross sections calculated from runs using targets of different thickness. A final error of 3% was assigned to the radiative correction procedure.

Extracting the structure functions from the measured cross section without performing a Rosenbluth separation requires a knowledge of the ratio of the absorption cross sections for longitudinal and transverse virtual photons, $R = \sigma_L / \sigma_T$. However, the error in extracting νW_2^A due to uncertainty in R is small for forward angles and for $R < 1$. We have assumed $R = 0.5/Q^2$ with an uncertainty of 50%, which is consistent with impulse approximation predictions as well as a recent measurement [9]. This leads to a worst case contribution to the uncertainty in νW_2^A of $\pm 3\%$. The

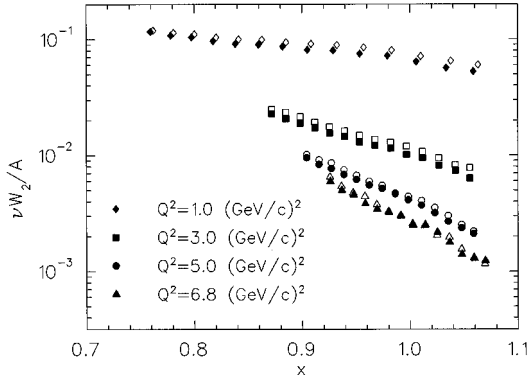


FIG. 2. $\nu W_2/A$ vs x for iron (solid points) and carbon (hollow points).

scaling function $F(y)$ was extracted from the measured cross section using the same method as Day *et al.* [8] and Potterveld [18].

The extracted scaling function $F(y)$ for iron is shown in Fig. 1, along with the previous SLAC NE3 data [8]. While the $y < 0$ data exhibited y scaling for the previous data, the scaling clearly breaks down at high Q^2 for all y values measured ($y > -80$ MeV/c). The breakdown of y scaling is due to the transition from quasielastic scattering to inelastic scattering. To test y scaling in this region, one must calculate and subtract off inelastic contributions to the cross section. This introduces a model dependence and can only be done reliably when the inelastic contributions do not dominate the cross section. It is clear that in the case of inclusive scattering, the applicability of y scaling is limited to lower momentum transfers, where quasielastic scattering dominates the cross section.

Figure 2 shows the measured structure function per nucleon for iron and carbon as a function of x . Clearly the data do not scale in this range but the Q^2 dependence is decreasing as Q^2 increases. The structure function is nearly identical for all of the nuclear targets except deuterium, where the smaller Fermi momentum causes a peak in the structure function near $x=1$. The larger Fermi momentum in the heavier nuclei washes out the quasielastic peak, leading to a lower structure function near $x=1$. The difference between carbon and iron decreases as x gets further from 1 and at higher Q^2 . Table I gives the ratio of the structure func-

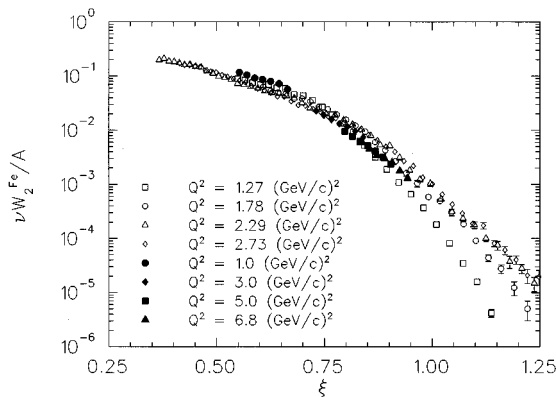


FIG. 3. νW_2^{Fe} vs ξ for the present experiment and the NE3 measurement.

TABLE I. Ratio of structure functions ($\nu W_2/A$) for different targets near $x=1$.

Q^2 [(GeV/c) ²]	C/Fe	Fe/Au	Fe/D
1.0	1.14±0.05	1.11±0.05	
3.0	1.14±0.05	1.19±0.05	0.48±0.03
5.0	1.07±0.05	1.16±0.05	0.69±0.04
6.8	1.05±0.05	0.96±0.05	0.95±0.06

tions for different targets at each Q^2 , for $0.95 < x < 1.05$, and the ratio of iron to deuterium for $x=1$. The Q^2 behavior of the ratio to deuterium is consistent with the behavior found for aluminum [15].

In Fig. 3, νW_2 is plotted vs ξ and an approach to scaling is observed. The new data are all centered at $x=1$, but move to higher ξ as Q^2 increases, lying on the universal curve. To better understand the transition, we calculated the contributions due to the different scattering processes using the convolution model of Ji and Filippone [17] with a Woods-Saxon spectral function, dipole electric form factor, and the magnetic form factor of Gari and Krümpelmann [16]. Figure 4 shows the approach to scaling for fixed ξ along with our calculations showing the quasielastic and deep inelastic contributions to the structure function. Also included is the NE11 data for aluminum [9], which are in good agreement when the structure function is scaled by the number of nucleons. As a function of Q^2 , we see an increase in the structure function on the low Q^2 side of the quasielastic peak, and then a decrease to the high Q^2 value, where inelastic scattering dominates. While the structure function is not independent of Q^2 for a fixed ξ , it shows less Q^2 dependence than when viewed at a constant x . More importantly, the measured structure function has relatively little Q^2 dependence in the region of transition from quasielastic to inelastic scattering, even though the quasielastic contribution is falling rapidly with Q^2 . This is true for all ξ values measured, indicating a connection between the quasielastic and inelastic cross sections, reminiscent of local duality in the nucleon.

To summarize, we have extracted the scaling function $F(y)$ and the structure function νW_2 near $x=1$ for nuclei with A ranging from 2 to 197 at Q^2 values from 1 to 6.8 (GeV/c)². At the higher Q^2 values, y scaling breaks down

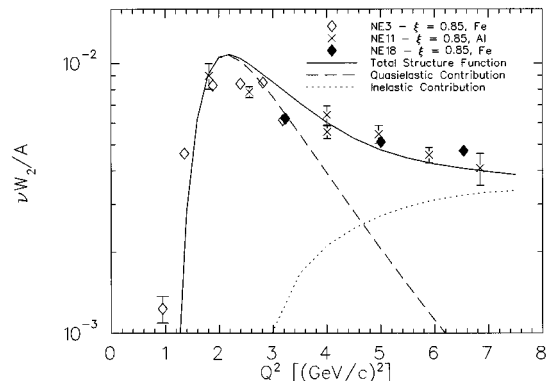


FIG. 4. νW_2^{Fe} is plotted vs Q^2 at $\xi=0.85$. The lines are calculations of the total (solid), quasielastic (dashed), and deep inelastic (dotted) contributions to the structure function.

for all measured values of y as deep inelastic scattering begins to dominate. When examining νW_2 , we do not yet see scaling in x , but we do begin to see scaling in the Nachtmann scaling variable ξ . This suggests a connection between quasielastic and inelastic scattering, similar to the case of local duality in the nucleon. ξ scaling may prove to be a useful tool in understanding nuclear structure functions, but better coverage in ξ at the present Q^2 values, as well as higher Q^2 measurements (e.g., at CEBAF [19]) are needed to fully understand the scaling of the structure function, and the relation between ξ scaling and y scaling.

This work was supported in part by the National Science Foundation under Grant Nos. PHY-9014406 and PHY-9114958 (American), PHY-9115574 (Caltech), PHY-9101404 (CSLA), PHY-9208119 (RPI), PHY-9019983 (Wisconsin), and by the Department of Energy under Contract Nos. W-31-109-ENG-38 (Argonne), DE-FG02-86ER40269 (Colorado), W-2705-Eng-48 (LLNL), DE-AC02-76ER03069 (MIT), DE-AC03-76SF00515 (SLAC), DE-FG03-88ER40439 (Stanford). R.G.M. acknowledges the support of the Presidential Young Investigator Award Program at NSF. B.W.F. acknowledges the support of the Sloan Foundation.

-
- [1] H. Georgi and H. D. Politzer, Phys. Rev. D **14**, 1829 (1976).
 [2] S. A. Gurvitz, Phys. Rev. D **52**, 1433 (1995).
 [3] G. B. West, Phys. Rep. **18**, 263 (1975).
 [4] I. Sick, D. B. Day, and J. S. McCarthy, Phys. Rev. Lett. **45**, 871 (1980).
 [5] B. W. Filippone *et al.*, Phys. Rev. C **45**, 1582 (1992).
 [6] E. Bloom and F. Gilman, Phys. Rev. D **4**, 2901 (1971).
 [7] A. DeRujula, H. Georgi, and H. D. Politzer, Ann. Phys. (N.Y.) **103**, 315 (1977). For a recent discussion of duality see C. E. Carlson and N. C. Mukhopadhyay, Phys. Rev. D **41**, 2343 (1990); **47**, R1737 (1993).
 [8] D. B. Day *et al.*, Phys. Rev. Lett. **59**, 427 (1987).
 [9] P. E. Bosted *et al.*, Phys. Rev. C **46**, 2505 (1992).
 [10] T. G. O'Neill, Ph.D. thesis, California Institute of Technology, 1994; T. G. O'Neill *et al.*, Phys. Lett. B **351**, 4775 (1995).
 [11] N. C. R. Makins *et al.*, Phys. Rev. Lett. **72** 1986 (1994).
 [12] S. Stein *et al.*, Phys. Rev. D **12**, 1884 (1975).
 [13] L. W. Mo and Y. S. Tsai, Rev. Mod. Phys. **41**, 205 (1969).
 [14] Yung-Su Tsai, SLAC Report SLAC-PUB-848, 1971.
 [15] L. L. Frankfurt, M. I. Strikman, D. B. Day, and M. Sargsyan, Phys. Rev. C **48**, 2451 (1993).
 [16] M. F. Gari and W. Krümpelmann, Z. Phys. A **322**, 689 (1985).
 [17] Xiangdong Ji and B. W. Filippone, Phys. Rev. C **42**, R2279 (1990).
 [18] D. H. Potterveld, Ph.D. thesis, California Institute of Technology, 1989.
 [19] D. B. Day and B. W. Filippone, CEBAF Proposal E89-008.